GEOPHYSICAL RESEARCH LETTERS, VOL. 35, L03111, doi:10.1029/2007GL032164, 2008

First radar measurements of ionospheric electric fields at sub-second temporal resolution

Raymond A. Greenwald,[1] Kjellmar Oksavik,[1,2] Robin Barnes,[1] J. Michael Ruohoniemi,[1] Joseph Baker,[1] and Elsayed R. Talaat[1]

Received 26 September 2007; revised 13 December 2007; accepted 14 January 2008; published 14 February 2008.

[1] A new multipulse sounding technique currently being used at the Wallops Island and Goose Bay SuperDARN radars has produced significant improvements in the temporal resolution of Doppler velocity measurements from which plasma velocities and electric fields are determined. The new technique allows Doppler velocities to be determined from every 200 ms multipulse sequence transmitted by the radar (equivalent to a 5 Hz measurement rate). To our knowledge, this is the highest Doppler measurement rate that has ever been attained with ionospheric radars. Tests of the new technique with the Wallops radar and Ottawa magnetometer revealed bursts of subauroral electric and magnetic field pulsations with periods of 13–20 s during a substorm expansion phase. These results indicate that SuperDARN measurements can be used to study highly dynamic processes in the coupled magnetosphere-ionosphere system, including storm and substorm electrodynamics, short-period pulsations and short-term variability in Joule heating. **Citation:** Greenwald, R. A., K. Oksavik, R. Barnes, J. M. Ruohoniemi, J. Baker, and E. R. Talaat (2008), First radar measurements of ionospheric electric fields at sub-second temporal resolution, *Geophys. Res. Lett.*, *35*, L03111, doi:10.1029/2007GL032164.

1. Introduction

[2] Over the years, many techniques have been used to measure plasma velocities and electric fields within the Earth's ionosphere. These two quantities are related to one another through the expression $\boldsymbol{E} = -\boldsymbol{V}_p \times \boldsymbol{B}$, where $\boldsymbol{V}_p$ is the plasma velocity transverse to the magnetic field, $\boldsymbol{B}$ is the magnetic field at the location of the measurement and $\boldsymbol{E}$ is the self-consistent electric field. Some techniques provide direct measurements of plasma velocities while others provide direct measurements of electric fields. Instruments used have flown on sounding rockets and spacecraft in low Earth orbit [e.g., *Pfaff et al.*, 1987; *Hanson et al.*, 1993] and on scientific balloons in the stratosphere [e.g., *Bering and Benbrook*, 1995]. Radars have provided measurements from the Earth's surface [e.g., *Banks et al.*, 1974; *Ruohoniemi et al.*, 1987]. In general, the space-based and balloon-based techniques have provided measurements with sub-second or higher temporal resolutions, whereas radars have provided measurements with temporal resolutions of 10's of seconds to 10's of minutes depending on the area of the ionosphere that is under investigation and the strength of the backscattered signals. Despite the lower temporal resolution, radars have provided measurements over extended regions of the ionosphere and the ability to determine the temporal evolution of plasma drifts and electric fields within their fields of view.

[3] An important question, however, is whether the temporal resolution of the radar observations is adequate to resolve fully all of the important physical processes in the region of observation. Processes where high temporal resolution electric field measurements are required include substorm-induced changes in ionospheric electric fields; Joule heating resulting from rapid changes in ionospheric electric fields; and magnetosphere-ionosphere coupling processes, including MHD waves, that produce rapid temporal variations of electric fields in the ionosphere.

[4] In this letter, we report on a recent advance in Doppler velocity determination with the Wallops Island and Goose Bay SuperDARN radars. This advance has been made possible through the development of a new multipulse transmission sequence that significantly improves the quality of autocorrelation functions (ACFs) derived from the backscattered radar signals and has allowed high quality Doppler measurements to be obtained from individual multipulse sequences. The technique has reduced the time required for the determination of the Doppler velocity from once every 3–7 seconds to 5 per second, an improvement of more than an order of magnitude over the highest temporal resolution achieved with SuperDARN to date. To our knowledge, this is the highest temporal resolution ever achieved with ionospheric radars. We can now study many highly dynamic processes in the subauroral, auroral, and polar cap ionospheres and investigate their impacts on the ionosphere, thermosphere, and magnetosphere. In this letter, we describe the new analysis technique and demonstrate it with the first radar observations of electric fields associated with short period (14–20 s) Pi 1 pulsations.

[5] We should note that this is not the first effort to study atmospheric and ionospheric phenomena at less than the integration time of the SuperDARN radars. Several years ago, *Yukimatu and Tsutsumi* [2002] reported on observations of meteor echoes with durations of 0.1–1.0 s that they were able to identify in the data samples from each integration period. Meteors are typically observed within the first few range gates of the radar and exhibit characteristic response patterns. One Doppler velocity measurement was derived for each meteor identified and typically utilized data from several multipulse sequences. The work of *Yukimatu and Tsutsumi* [2002] used the traditional SuperDARN multi-

[1] Johns Hopkins University Applied Physics Laboratory, Laurel, Maryland, USA.
[2] Now at University Centre in Svalbard, Longyearbyen, Norway.

0094-8276/08/2007GL032164$05.00

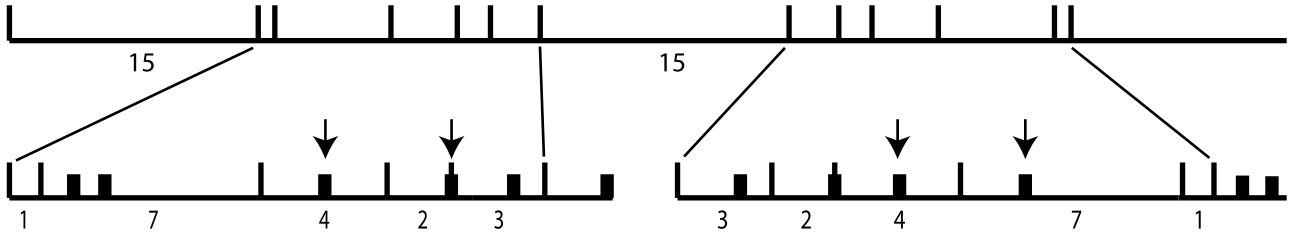

Figure 1. The top trace shows the new 13-pulse sequence used to produce improved autocorrelation functions with the Wallops Island and Goose Bay SuperDARN radars. The sequence consists of a single pulse to determine the profile of the backscattered signals and forward (bottom left trace) and reversed (bottom right trace) 6-pulse optimal sequences that mitigate interference from transmitter pulses and returns from unwanted ranges. The numbers represent lags between transmitter pulses. In the bottom traces, the tall narrow pulses represent transmitter pulses and the short wide pulses represent backscattered returns. The downward pointing arrows above the lower traces indicate periods when backscattered signals are detected. In the left hand trace, the second sample of data is unusable since it is received during a transmitter pulse. This does not occur for the reversed sequence shown in the right hand trace. See text for further details.

pulse patterns and would benefit from the advanced multipulse patterns that we report here.

2. Advanced Multipulse Analysis Technique

[6] The use of multipulse sequences for radar applications was first suggested by *Farley* [1972] as a means of determining unambiguously the autocorrelation function (ACF) and spectral properties of backscattered signals as a function of range. Since that time the multipulse technique has been widely used in incoherent scatter radar applications [e.g., *Rino et al.*, 1977] and in SuperDARN [e.g., *Greenwald et al.*, 1985]. Although multipulse sequences have desirable properties, they also have shortcomings because they introduce considerable unwanted noise to the analysis. This occurs when transmitter pulses and/or backscattered signals from unwanted ranges overlap data being analyzed and render one or more lags of the desired ACF unusable. The new approach is based on a previously unrecognized property of multipulse sequences that, if utilized, greatly reduces the impact of this undesirable noise and produces ACFs with larger numbers of good lags.

[7] Multipulse sequences are based on the mathematical concept of "Golomb Rulers" (available at http://en.wikipedia.org/wiki/golomb_ruler). In the mathematical sense, the objective is to identify the minimum pattern of marks that are needed on a ruler to measure all integer distances (i.e. 1,2,3,. . ..) and not have any distance measured more than once. In the radar case, the objective is to identify the minimum pattern of transmitted pulses that are needed to determine all lags of an ACF. In reality, there are no perfect rulers or multipulse sequences with more than four marks or transmitter pulses. There will always be missing distances (lags). However, there are sequences that are optimal [see *Farley*, 1972] and we have chosen to adopt one of these as the basis for our new multipulse transmission sequence.

[8] The new multipulse transmission sequence being used at the Wallops Island and Goose Bay radars is shown in Figure 1. The top trace shows the full transmission sequence which is comprised of 13 transmitter pulses. The signal returns from the first transmitted pulse are used to determine the strength of the backscattered signals as a function of range from the radar. Knowledge of this profile is important if one wants to maximize the benefits of the new multipulse sequence. Profile measurements are typically made to a range of 4600 km. The next 6 transmitted pulses represent one of the multipulse sequences identified by *Farley* [1972]. A blow-up of this sequence is represented by the tall and narrow pulses in the bottom left of the figure. The sequence has gaps of 1, 7, 4, 2, and 3τ between transmitter pulses, where τ is the minimum time separation between transmissions. This sequence is an optimal ruler. The only gaps that cannot be measured are 10τ and 15τ. The final six pulses in the upper trace represent the same Farley sequence in reverse order. These are expanded at the bottom right of Figure 1. This sequence is separated from the first sequence by 15τ as is the first sequence from the initial transmitted pulse. Thus with the exception of 10τ, there are two possible alternative choices for all lags of the ACF from τ to 17τ.

[9] We shall now see how the use of reversed nonredundant multipulse sequences mitigate interference from transmitter pulses and unwanted noise in multipulse Doppler measurements. The short wide pulses in the lower traces of Figure 1 represent backscattered returns from each of the transmitted pulses. Note that they occur at a fixed delay following each transmission. The downward pointing arrows identify two of these returns that are associated with transmitter pulses separated by 4τ in each of the forward and reversed sequences. Careful examination of the bottom trace to the left shows that the backscattered signals due to the second transmitter pulse are received at the same time as another pulse is transmitted. Since monostatic radars cannot transmit and receive at the same time, these data are unusable and cannot contribute to the ACF determination. However, the same backscattered signals in the trace at the bottom right are unaffected by transmitter pulses and therefore yield good measurements. The interested reader may confirm that each sequence has 5 bad lags at this delay. Together the two sequences have 9 bad lags, but only lag 2τ is bad for both sequences. Thus, by using forward and reverse sequences, the researcher can reduce the number of bad lags in the ACF from 5 to 1. Similar arguments that we do not report here show that strong backscatter returns from unwanted ranges cause similar problems and since they occur at a specific delay following each transmitter pulse, they can be mitigated by forward and reverse sequences.

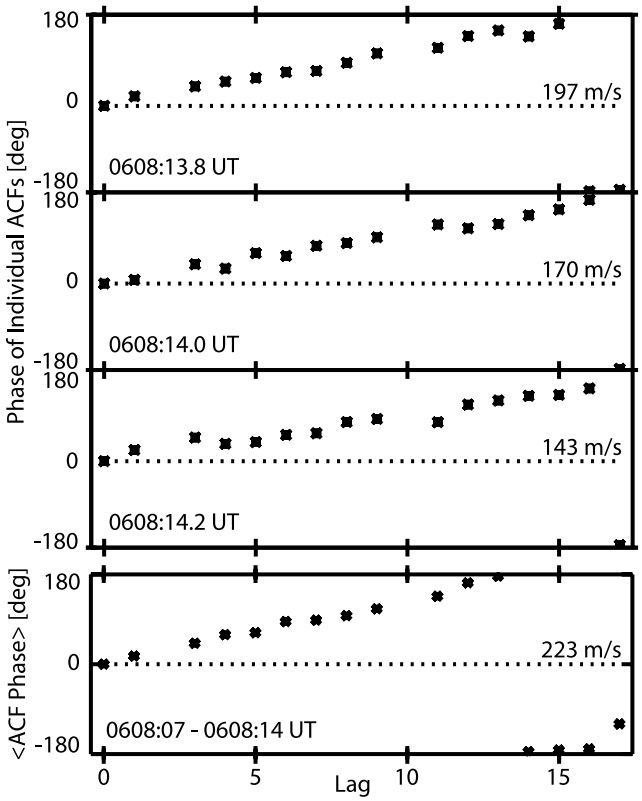

Figure 2. Phase versus lag profiles of data obtained on 1 August 2007 at the Wallops Island radar. The top 3 panels show the phase versus lag profile of ACFs at a fixed range derived from backscatter returns for three sequential multipulse sequences. The Doppler velocity is determined from the phase slope and is indicated at the right of each panel. The bottom panel shows the median phase slope for 7 seconds of data on the same beam and range. Note that the phase noise of the individual sequences and the 7 s median are comparable.

[10] The new multipulse sequence shown in Figure 1 requires slightly more than 200 ms for transmission and reception of the data. Over a 7 s integration time, approximately 33 sequences are transmitted and received and either a mean or median fit to the resulting complex ACFs is determined. The Doppler velocity is derived from a least squares fit to the slope of the time-dependent phase of the backscattered signal defined as:

$$\langle \varphi(n\tau, r) \rangle = \tan^{-1} \left(\langle \mathrm{ACF}_{\mathrm{imag}}(n\tau, r) \rangle / \langle \mathrm{ACF}_{\mathrm{real}}(n\tau, r) \rangle \right)$$

where $\langle\rangle$ denotes mean or median, τ is the minimum lag of the multipulse sequence (i.e. the inverse of the sampling frequency at any particular range), n is the lag number, ϕ is the phase of the ACF at lag $n\tau$, and r is the range to the ionospheric region under investigation.

[11] During the development of the new sequence, all receiver samples were saved as raw sample files at the Wallops radar site so that the new processing technique could be evaluated retrospectively and refined in a controlled manner. As part of this evaluation process, ACFs were determined for individual multipulse sequences and their phases were plotted as a function of lag. The top three panels in Figure 2 were obtained from three sequential multipulse sequences separated by slightly more than 200 ms. Each sequence is labeled with a Doppler velocity determined from a least squares fit to the measured phases. It can be seen that the velocity is steadily decreasing at $\sim$27 m/s per sequence or $\sim$135 m/s^2. The bottom panel in Figure 2 was obtained from the median values of the complex ACF for the 7 s integration (33 multipulse sequences). Note that the median value of the Doppler velocity was 223 m/s and that the phase scatter of the data points in the median slope is comparable to the phase scatter of the data in the individual sequences. Also note that in these examples all lags are present with the exception of the missing lag 10τ and lag 2τ. The latter lag corresponds to the range gate shown in Figure 1 that lies on a transmitter pulse.

[12] It should be quite clear from Figure 2 that the data samples from a single multiple sequence are capable of yielding quality Doppler velocity measurements at a rate of 200 ms per observation (5 Hz). There are, however, two minor caveats. First, the data samples must be saved at the radar for retrospective analysis. The analysis is computationally intensive and cannot be done in real time. Second, the procedure requires good signal to noise ratios (SNR) ($\sim$7–10 dB) for the phase scatter to be as small as shown in the upper panels of Figure 2. Ranges with lower SNR will exhibit more phase scatter, but may still yield Doppler measurements of acceptable quality.

3. High-Temporal Resolution Velocity Measurements with the Wallops Radar

[13] We now present a more extended view of the data shown in Figure 2. These data were obtained shortly after 06 UT on 1 August 2007 during a disturbed Kp = 4 period in which there were several substorm intensifications. The Wallops radar was in the post-midnight sector at $\sim$02 MLT. The measurements we report were made in the subauroral ionosphere $\sim$200 km west of the Ottawa magnetometer operated by the Geological Survey of Canada. Both the radar and magnetic observations were made in the subauroral ionosphere at $\Lambda \approx 57^\circ$. Figure 3a shows a dynamic wavelet power spectrum of the power in the Pi 1 band as determined from the X-component of the Ottawa magnetometer for the time period 0604–0611 UT on 1 August 2007. It can be seen that the spectrum is both dynamic and rich in frequency content during this period. Some features to note are the 20 s pulsation that began at $\sim$0605 UT and continued to 0630 UT, the 13 s pulsation that started at $\sim$0607:20 UT and continued to 0608:20 UT, and the 28 s pulsation that began at $\sim$0608 UT and continued to 0609:40 UT.

[14] Figure 3b shows high-temporal resolution Doppler measurements from the Wallops radar for the time period from 0604–0611 UT. The radar was scanned through 16 beam directions with backscattered signals from the subauroral F-region ionosphere being observed continuously on 4–7 range gates for each of the most poleward 5–6 beam directions throughout the midnight sector. These beam directions were clustered about 21° east of geographic north. The observations showed no systematic range depen-

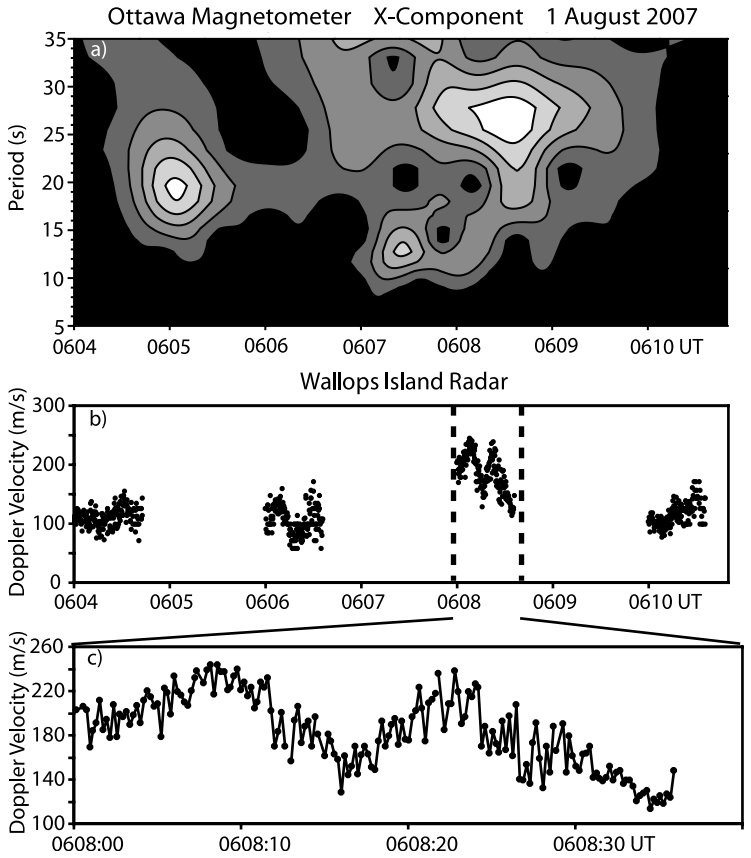

Figure 3. (a) Wavelet analysis of Pi 1 pulsations observed in the X-component of the Ottawa magnetometer between 0604–0611 UT on 1 August 2007. The contour levels indicate relative spectral power of 0.25 (black), 1, 2, 3, and 4 (white). The strongest Pi 1 pulsations are observed at periods of 13, 19, and 27 s. (b) Unfiltered time series of high temporal resolution Doppler velocity measurements from the Wallops Island radar for the same period. (c) Detailed view of the large amplitude velocity oscillation for the period 0608:00–0608:36 UT. The periodicity of the initial half of this oscillation is very similar to that observed from the wavelet analysis.

dence so all Doppler velocities derived from each multipulse sequence have been averaged to yield a mean Doppler velocity for each 200 ms interval. We also found that the data exhibited temporal continuity as the radar was scanned from one beam direction to the next. Noting this, we have simply plotted the data as a continuous time series of Doppler measurements, rather than trying to project the Doppler measurements into some assumed flow direction. Because of the relatively small angle between geographic north and the beam pointing directions, north-south drifts dominate east-west drifts in the Doppler measurements as long as the two drifts are of comparable magnitude. Therefore, we assume that we are observing approximately north-south plasma velocity oscillations driven by east-west oscillations in the ionospheric electric field.

[15] Forty-two seconds of data are plotted for the 0604 UT scan and 35 seconds of data are plotted for each of the remaining scans. The gaps between the data occur as the radar is scanned toward lower geomagnetic latitudes where no ionospheric backscatter was observed. This is either due to an absence of irregularities in these viewing directions, or to the radar signals undergoing insufficient ionospheric refraction to achieve orthogonality with the irregularities that are present.

[16] A strong pulsation in the Doppler velocity is easily seen during the 0608 UT scan in Figure 3b. The oscillation in the plasma drift had a maximum peak-to-peak amplitude of 80 m/s (equivalent to a peak-to-peak electric field oscillation of 4 mV/m). This pulsation is expanded in Figure 3c and clearly shows evidence of the 13–14 s periodicity that is observed in the Ottawa wavelet analysis.

[17] It is also interesting to note that the 0608 UT pulsation occurred while there was a 100 m/s short-lived enhancement in the quasi-DC component of the plasma drift. This quasi-DC enhancement is only seen during the 0608 UT scan and may itself have been associated with the 28 s pulsation that was identified in the Ottawa wavelet analysis at this time.

[18] Evidence of another pulsation is readily seen in the 0606 UT scan. This pulsation is weaker and appears to have a period of ~20 s that may be related to the 20 s pulsation seen in the Ottawa wavelet analysis. The scans at 0604 UT and 0610 UT also show some evidence of pulsations but will not be discussed further at this time.

[19] One interesting point to note is that the wavelet analysis suggests that both the 20 s and 13 s pulsations may have been strongest when the Wallops radar was directed away from the region of interest. It would appear to be quite valuable scientifically, if an extended time series

of high temporal resolution observations were available in conjunction with high temporal resolution magnetic observations from one or more magnetometers sites.

4. Summary

[20] In this letter, we have described a new multipulse sounding sequence that substantially reduces the noise inherent in multipulse sounding techniques and greatly improves the temporal resolution of SuperDARN Doppler velocity measurements. Previously, the best temporal resolution attained with SuperDARN was 3 s integrations. With the new technique, Doppler measurements can be derived from each of the new 200 ms multipulse sequences. The new technique extends the applicability of SuperDARN velocity and electric field measurements to many new areas of research including short period pulsations, storm and substorm dynamics, and short-term variability in Joule heating. It may lead to improved understanding of velocity turbulence in the ionosphere.

[21] We have demonstrated the success of the new multipulse analysis technique by showing that the Wallops radar is capable of detecting very short period electric field pulsations in the subauroral ionosphere. The peak-to-peak amplitude of these pulsations ranged from 2–4 mV/m and the periods ranged from ~14–20 seconds. Magnetic field pulsations with similar periods and peak-to-peak amplitudes of 1–2 nT were observed concurrently with the nearby Ottawa magnetometer.

[22] Although the Doppler measurements reported here were limited to a few scans of the Wallops Island radar, the results demonstrate the potential of the higher temporal resolution plasma velocity and electric field measurements that are now available. The data set we presented was intermittent because the Wallops radar was being scanned and only certain beam directions detected backscatter from ionospheric irregularities. Fortunately, many SuperDARN radars are currently able to collect data in two operating modes concurrently. It is therefore possible to perform SuperDARN azimuth scans to allow large area coverage while simultaneously performing continuous measurements along a fixed viewing direction. This will allow continuous coordinated measurements between SuperDARN radars and magnetometers or other ground based instrumentation.

[23] **Acknowledgments.** We would like to thank the Geological Survey of Canada Geomagnetic Survey Network for providing high-temporal resolution data from the Ottawa magnetometer for use in this study. Support for this work was provided by the National Science Foundation Upper Atmosphere Facilities Program under Grant ATM-0418101 and NASA Grant NNX06AB95G.

References

Banks, P. M., C. L. Rino, and V. B. Wickwar (1974), Incoherent scatter radar observations of westward electric fields and plasma densities in the auroral ionosphere, *J. Geophys. Res.*, *79*, 187–198.

Bering, E. A., and J. R. Benbrook (1995), Intense 2.3-Hz electric field pulsations in the stratosphere at high auroral latitudes, *J. Geophys. Res.*, *100*, 7791–7806.

Farley, D. T. (1972), Multi-pulse incoherent scatter correlation function measurements, *Radio Sci.*, *7*, 661–666.

Greenwald, R. A., K. B. Baker, R. A. Hutchins, and C. Hanuise (1985), An HF phased-array radar for studying small-scale structure in the high-latitude ionosphere, *Radio Sci.*, *20*, 63–79.

Hanson, W. B., W. R. Coley, R. A. Heelis, N. C. Maynard, and T. L. Aggson (1993), A comparison of in situ measurements of E and $-VxB$ from Dynamics Explorer 2, *J. Geophys. Res.*, *98*, 21,501–21,516.

Pfaff, R. F., M. C. Kelley, E. Kudeki, B. G. Fejer, and K. D. Baker (1987), Electric field and plasma density measurements in the strongly driven daytime equatorial electrojet: 1. The unstable layer and gradient drift waves, *J. Geophys. Res.*, *92*, 13,578–13,596.

Rino, C. L., A. Brekke, and M. J. Baron (1977), High-resolution auroral zone E region neutral wind and current measurements by incoherent scatter radar, *J. Geophys. Res.*, *82*, 2295–2304.

Ruohoniemi, J. M., R. A. Greenwald, K. B. Baker, J.-P. Villain, and M. A. McCready (1987), Drift motions of small-scale irregularities in the high-latitude F region: An experimental comparison with plasma drift motions, *J. Geophys. Res.*, *92*, 4553–4564.

Yukimatu, A. K., and M. Tsutsumi (2002), A new SuperDARN meteor wind measurement: Raw time series analysis method and its application to mesopause dynamics, *Geophys. Res. Lett.*, *29*(20), 1981, doi:10.1029/2002GL015210.

J. Baker, R. Barnes, R. A. Greenwald, J. M. Ruohoniemi, and E. R. Talaat, Johns Hopkins University Applied Physics Laboratory, 11100 Johns Hopkins Road, Laurel, MD 20723, USA. (ray.greenwald@jhuapl.edu)

K. Oksavik, University Centre in Svalbard, PB 156, NO-9171 Longyearbyen, Norway.